Studies of Higher Temperature Polymerization of *n*-Butyl Methacrylate and *n*-Butyl Acrylate

Michael C. Grady[a]*, *William J. Simonsick*[a] *and Robin A. Hutchinson*[b]

[a]DuPont Company, Marshall Laboratory, Philadelphia, PA, USA
[b]Department of Chemical Engineering, Queen's University, Kingston, Ontario, Canada

Summary: Free-radical acrylic polymerizations of n-butyl methacrylate and n-butyl acrylate at temperatures above 120 °C show significant departure from classic free-radical kinetics. An extended model of depropagation, where the equilibrium monomer concentration varies with temperature and polymer content, is postulated and shown to adequately explain the data for n-butyl methacrylate. Intramolecular chain transfer and scission is postulated to explain the apparent reduction in molecular weight and rate of polymerization seen in n-butyl acrylate polymerization, with supporting experimental evidence found via electrospray-ionization mass spectrometry.

Introduction

North American regulations[1-3] on volatile organic content (VOC) of coatings will reduce allowable VOC's from 480 g/L of paint in 1990 to below 300 g/L by 2010. These and similar regulations[4,5] are driving change in the basic nature of resin in coatings. Low molecular weight, highly functionalized polymer and oligomer solutions at 60 to 80 weight percent solids[6] have replaced high molecular weight, non-functional polymer solutions at 30 to 40 weight percent solids as key components in coatings formulas. Molecular weight control is achieved in a variety of ways and unfortunately each method can detract from the end use properties of the coating. One method is to increase the amount of free-radical initiator relative to monomer on formula.[7] This reduces the molecular weight of the resin but adds cost as initiators are normally the most expensive component of a formula. It also increases the safety risk of handling concentrated initiator solutions[8] and makes dissolution of solid initiators more difficult. A second method is to use chain transfer agents like mercaptans, reversible addition fragmentation agents,[9] cobalt porphyrin complexes,[10] nitroxide mediated polymerization catalysts,[11] or atom transfer radical catalysts[12] but these invariably leave a moiety in the solution or attached to the polymer chain that can cause difficulty later in the coating application. For example, mercaptans have an offensive smell and the sulfur is known to reduce long term durability.[13] Cobalt glyoximes impart a dark, reddish color to the resin limiting their usefulness in clear-coat formulations, and the

 CCC 1022-1360/00/$ 17.50+.50/0

cobalt species can also catalyze post-reactions of the resin solution. Nitroxide and other controlling agents can slow polymerization rates and limit complete conversion of monomer to polymer. A third way to control molecular weight is to polymerize at temperatures greater than ca. 120 °C[14] to yield low molecular resin at reasonable initiator levels without the use of chain transfer agents. This method also has drawbacks, including higher energy consumption and higher rates of competing side reactions that can detract from final coating properties. Some side reactions, such as the rearrangement of hydroxyl functionality from secondary to primary, change the reactivity of the functionalized polymer, affecting film curing rates and coating properties. Other secondary reactions, the focus of this work, impact the polymerization rate and polymer molecular weight and structure. Nonetheless, high temperature polymerization is often the most attractive alternative: it is easy to implement and adds no additional moieties to the polymer chain or into the polymer solution.

Molecular weight distribution and monomer conversion in higher temperature polymerization depart significantly from those predicted by classic free-radical kinetics. The most basic of process parameters, such as feed time in a semi-batch process (or residence time in a continuous stirred tank reactor) and polymer content have a significant impact on the resulting polymer properties. Table 1 shows this influence on weight average molecular weight (M_w) for two different copolymers. This data is typical of industrial polymerizations taken to near complete conversion. The theoretical predictions in Table 1, made using a classic kinetic model that includes initiation, propagation and termination, clearly do not match the experimental findings. Proper design and safe industrial operation of such polymerizations require a better understanding of high-temperature free-radical kinetics. Additional mechanisms are needed to explain the strong influence of these simple process parameters on the resulting polymer characteristics. Possible mechanistic explanations include: (1) thermal initiation of monomer;[15-17] (2) initiator efficiency[18,19] and/or termination rate constants[20,21] changing with polymer content in the reactor; (3) methacrylate depropagation;[22-24] and (4) acrylate branching and scission reactions.[25,26] Thermal initiation of these monomers is negligible below 200 °C, especially when compared with the high level of initiator used, and viscosity of these low-M_w polymer solutions remains under 50 centipoise at reaction temperature, suggesting that the rate of diffusion controlled reactions will vary little. Thus we focus our attention on the remaining two explanations – methacrylate depropagation and acrylate branching and scission.

Table 1. The Impact of Simple Semi-Batch Process Parameters on M_w

Case 1[a]	*Feed Time*	*Experimental*	*Theoretical*
	hours	M_w	M_w
	4	12100	11234
	8	5450	11292
Case 2[b]	*Final Polymer*	*Experimental*	*Theoretical*
	Content %	M_w	M_w
	40	4276	9600
	70	10477	10100

[a] 50/50 nBA/BMA copolymer made with a semi-batch process using refluxing xylene (ca. 140 °C) as solvent and t-butyl peroxyacetate as initiator. Final solution polymer content at 75 %.

[b] 60/40 BMA/hydroxypropyl acrylate copolymer made with a semi-batch process using refluxing xylene as solvent and t-butyl peroxyacetate as initiator. Feed time held fixed at 7 hours.

Depropagation in methacrylate polymerization has been known for some time and studied extensively by Dainton and Ivin,[27,28] Bywater,[29] and others.[30-32] They described the basic premise that propagating methacrylate radical chains ($P_n^\bullet$) unzip with increasing frequency at higher temperature:

$$P_n^\bullet + M \underset{k_{dep}}{\overset{k_p}{\rightleftarrows}} P_{n+1}^\bullet$$

This reaction is thermodynamically controlled and the ratio of the forward to reverse rate constants is given by the equilibrium constant, $K = k_p/k_{dep}$ where $K = [M]_{eq}^{-1}$ and $[M]_{eq}$ is the equilibrium monomer concentration at a given temperature. There are two ways to consider the relationship between equilibrium monomer concentration and temperature.[33] The first considers monomer concentration to be fixed and defines T_c as the ceiling temperature at which net polymerization rate R_p tends to zero:

$$\text{at a given} [M], \lim_{T \to T_c} R_p \to 0$$

The second considers temperature to be fixed and defines $[M]_{eq}$ as the equilibrium monomer concentration below which polymerization will not proceed:

$$\text{at a given } T, \lim_{[M] \to [M]_{eq}} R_p \to 0$$

The approaches are equivalent: for a given ceiling temperature there exists an equilibrium monomer concentration and vice-versa. Bywater[29] used the equilibrium monomer concentration approach for a series of methyl methacrylate batch polymerizations starting at different initial monomer concentrations at constant

temperature. The data showed that, no matter the initial monomer concentration, each polymerization equilibrated at the same monomer concentration ($[M]_{eq}$) for a given temperature. When the initial monomer concentration was below this equilibrium value the polymerization did not proceed. More recently, Hutchinson et al. used a kinetic approach, measuring the Arrhenius coefficients for depropagation with a pulsed laser polymerization technique.[23] Most studies of depropagation have assumed the equilibrium monomer concentration to be dependent on temperature only. A recent review article by Ivin[22] alludes to the influence polymer content might have on thermodynamic equilibrium. In this paper we extend Bywater's approach to semi-batch polymerization of n-butyl methacrylate, and also demonstrate that polymer content has a significant effect on $[M]_{eq}$.

Depropagation does not occur in acrylate systems, but other secondary reactions play an important role. A concensus is emerging that H-abstraction and scission mechanisms have a significant impact on both polymerization rate and molecular weight, especially at higher temperature conditions. Low temperature pulsed-laser polymerization (PLP) measurements indicate a much higher propagation rate coefficient (k_p) for alkyl acrylates over those of the corresponding alkyl methacrylates.[34] Despite repeated efforts, however, PLP has been successfully applied only to acrylate systems below 30 °C and relatively high monomer concentrations.[35] Extrapolating the low temperature PLP data for n-butyl acrylate to 140 °C gives a k_p of 1.3×10^5 $mol\cdot L^{-1}\cdot s^{-1}$ which is about 35 times that of the propagation rate constant for n-butyl methacrylate. It has been shown that extrapolations of the PLP-determined k_p values do not represent higher temperature rate data.[26] The discrepancy has been explained by invoking a more complex set of mechanisms that include intramolecular hydrogen abstraction and slower propagation of the resulting mid-chain radical.[26,35-36] The plausibility of this proposal is supported by other experimental studies showing that hydrogen abstraction from acrylate units on a chain backbone occurs readily, leading to both short chain branches[37] and long chain branches;[38] the presence of mid-chain acrylate radicals has also been detected by ESR.[36] In addition to its effect on rate, the mid-chain radical has been shown to be capable of beta-scission fragmentation into a macromonomer and a smaller beta-scission radical,[25,36] thus affecting polymer molecular weight. In this work ^{13}C NMR and electrospray ionization – Fourier transform mass spectroscopic techniques are used to characterize polymer structure in order to determine the relative importance of these mechanisms.

Experimental Part

n-Butyl acrylate (nBA), inhibited with 50 ppm of methyl ether of hydroquinone, was obtained commercially from BASF at 99.5% purity and used as received. n-Butyl methacrylate (BMA), inhibited with 20 ppm of methyl ether of hydroquinone, was obtained commercially from INEOS at 99.0% purity and used as received. An isomeric xylene mix with a atmospheric boiling point range between 137 °C and 143 °C was obtained from ExxonMobil Chemical and used as received. The initiator, a 75% solution of t-butyl peroxyacetate (TBPA) in mineral spirits, was obtained commercially from Atofina Chemicals, stored in a 10 °C refrigerator and used as received. Semi-batch process runs were carried out in a 5 liter round-bottom flask fit with a dual-blade agitator and reflux condenser. In a semi-batch run[39] solvent is added to the reactor, heated to reflux at ca. 140 °C, and monomer and initiator solutions are cocurrently fed to the reactor at fixed rates over fixed time intervals. The base case formula is shown in Table 2. The process was controlled using a Camile Control and Data Acquisition system with automatic feed and temperature control.

Table 2. Formula for Base Case with 70 wt% Monomer and 400 min -Feed Time

I. Initial charge to purged reactor, heated to boiling at ca. 140 °C	
xylene	0.186
II. Monomer Feed over 400 minutes (Fed concurrently with Part III)	
BMA[a]	0.751
xylene	0.009
III. Initiator Feed over 415 minutes (Fed concurrently with Part II)	
TBPA	0.015
xylene	0.038
	1.000

[a] Wt fraction reduced to 0.70 after final reactor rinse; hence the title "70 wt % monomer"

Samples were drawn from the reactor at specified times and diluted 50/50 v/v in a cold 1000 ppm methyl ether of hydroquinone inhibitor solution to stop further reaction. Polymer content was determined by gravimetry on dried samples. Liquid samples were analyzed for residual monomer using a Hewlett Packard (Palo Alto, CA) 6890 gas chromatograph (GC) equipped with a flame ionization detector set at 250 °C. A 30m DB-5 column was used for separation, with temperature ramped to 250 °C at 10 °C /min after an initial 2.15 min hold at 50 °C. The column was held at 250 °C for an additional 2.85 min affording a total run time of 25 min. Molecular weight distributions were

determined using a Hewlett Packard (Palo Alto, CA) 1090 high performance liquid chromatograph equipped with a Hewlett Packard 1047A refractive index detector. The column set employed for the studies was a four column set consisting of 10^5 Å, 10^4 Å, 10^3 Å and 10^2 Å 30 cm × 7.8mm id Microstyragel columns (Waters, Milford, MA). Tetrahydrofuran (THF) at 40 °C was used as the mobile phase at a flow of 1mL/min. Data from the RI detector was collected and processed using a Waters Millennium system. Narrow molecular weight polystyrene (PS) standards were used to calibrate the column set, with MW values adjusted according to the mass spec analysis described below. While PS calibration provided reasonable accuracy for the low-MW nBA polymers produced in this study, the PS-calculated MW values for the BMA polymers were increased by 30% to give a more accurate measure of their true MW.

For the gel permeation chromatography (GPC) coupled with electrospray ionization Fourier transform mass spectrometry (GPC/ESI/FTMS) studies, GPC analysis was carried out using a four-column set of two 10^3 Å, 500 Å, and 100 Å 30 cm × 7.8 mm id Ultrastyragel columns (Waters, Milford, MA). The THF mobile phase was delivered by a Hewlett Packard (Palo Alto, CA) Model 1050 gradient liquid chromatograph at 1.0 mL/min, with polymer dissolved in the mobile phase at ~1% w/v. Effluent splitting was achieved with a T-junction (Valco) that supplied about 10 μL/min flow to the ESI source, with the remainder going to a Hewlett Packard Model 1037E refractive index detector. For post-column salt addition necessary for ionization, a sheath liquid (50 μM NaI in methanol) was delivered to the ESI tip by a Cole-Parmer 74900 series syringe pump operated at 10 μL/min. The Analytical ESI source (Branford, CT) fitted with a triple sheath needle assembly was interfaced to the Finnigan FT/MS Newstar system. The time resolved mass spectra, 128 K data points per spectrum, recorded above m/z = 300 were collected every second and the MS data processed by a Finnigan FT/MS Odyssey (Version 4.0) data system with the Charisma chromatography software package. Data from the RI detector was collected and processed using a Waters (Milford, MA) Millennium system. The selected oligomer profiles of the BMA or BA were used as the column calibrants.[40] Some samples were further analyzed using ^{13}C NMR using procedures and peak assignments similar to those described by Ahmad et al.[38] The experimental plan used in this work for the semi-batch process was a simple 2×2 grid with factors of feed time at levels of 180 minutes and 400 minutes and final polymer solids at 35 and 70 wt % polymer. Initiator level in the semi-batch process was held fixed at 2.0 wt % on monomer.

Results of the BMA Experiments

In the semi-batch polymerization of the base case the batch reflux temperature increases with increasing polymer content from ca. 140 °C to 148 °C over the course of the feeds as polymer content builds in the reaction mass. Figure 1 shows the M_w profiles of the 2×2 set of experiments. The base case line represents an average of three 400 min feed time, 70 wt % monomer experiments.

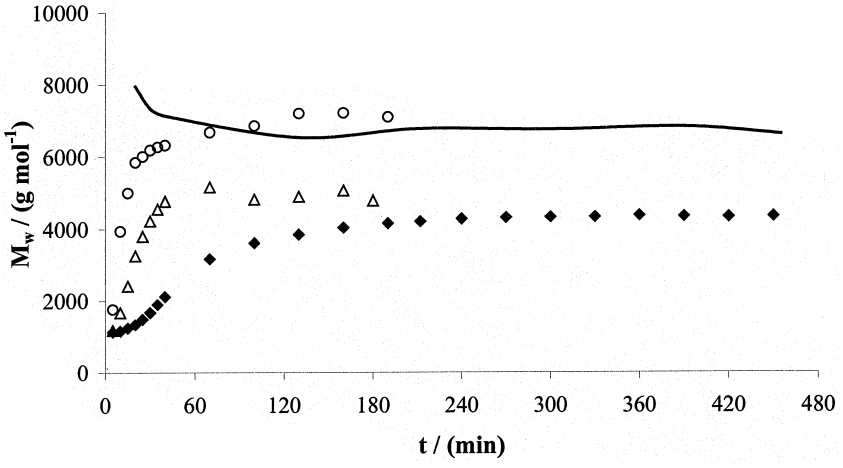

Figure 1. BMA weight average molecular weight profiles: 180 min feed, 70 wt % monomer (o); 180 min feed, 35 wt % monomer (Δ); 400 min feed, 35 wt % monomer case (♦); 400 min feed, 70 wt % monomer base case (——, average of 3 experiments).

Consistent with the data of Table 1, longer feed times and reduced final polymer content (i.e. reduced monomer content in the feed) lower molecular weight. The influence of polymer content is especially strong, with the lower monomer level reducing M_w by almost 50%. Figure 2 shows the unreacted monomer level for the two experiments employing 400 minute feeds at two different levels of polymer content. The free monomer level of the 35 wt % monomer formula is the higher of the two profiles. This is counter to intuition: one would expect higher monomer content in the feed to yield higher unreacted monomer level in the reactor. This data is strong evidence of the impact polymer content has on equilibrium monomer concentration profile. Figure 3 shows the same data for the 180 minute feed cases. The lower polymer content

experiment gives higher unreacted monomer levels in the reaction mass. For all four cases, the initial peak in unreacted monomer occurs at ca. 0.7 mol·L^{-1}.

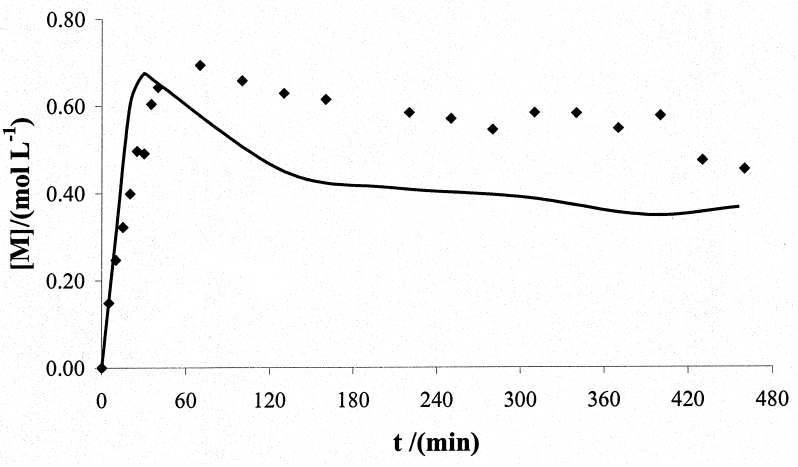

Figure 2. Unreacted BMA concentration profiles of the 400 min feed time experiments: 35 wt % monomer (♦); 70 wt % monomer base case (——).

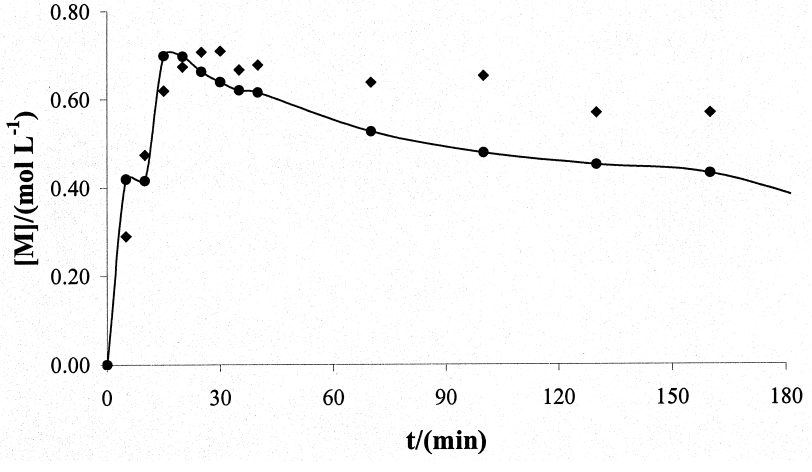

Figure 3. Unreacted BMA concentration profiles of the 180 min feed time experiments: 35 wt % monomer (♦); 70 wt % monomer (—●—).

Discussion of the BMA Results

The presence of polymer in a solution influences vapor-liquid equilibrium not only by the addition of a non-volatile species but also by changing the solvent activity in solution.[41] Likewise, in reaction equilibrium the presence of polymer can influence the equilibrium monomer content in the reaction mass. To show this relative to the BMA data acquired, one has to extend Bywater's solution[29] of the equilibrium monomer concentration for a batch process to semi-batch polymerization. Solving the monomer balance by using the equilibrium relationship $k_p[M]_{eq} = k_{dep}$ and substituting $\tau(t) = V(t)/q$ gives (q = volumetric feed rate; V = volume; M_f = monomer concentration in feed; $[P^\bullet]$ = radical concentration in reactor):

$$[M] = \frac{\left(M_f + k_p[M]_{eq}[P^\bullet]\tau\right)}{\left(1 + k_p[P^\bullet]\tau\right)} e^{-\left[\left(1+k_p[P^\bullet]\tau\right)\left(t/\tau\right)\right]} \tag{1}$$

Figure 4 shows the $[M]$ profiles calculated for a 140 °C semi-batch BMA polymerization for a series of different equilibrium monomer concentrations, with rate constants taken from the literature.[42-45] $[M]$ builds to a value greater than $[M]_{eq}$ and then decays back towards $[M]_{eq}$ over the course of the feeds. In Figure 4 the experimental data for the base case is also presented. The experimental profile crosses through the family of calculated curves, suggesting that $[M]_{eq}$ changes with time during the experiment. This result can be understood by thermodynamic arguments: just as polymer influences solvent activity for vapor-liquid equilibrium, it also influences monomer activity and reaction equilibrium. The equilibrium constant for the propagation - depropagation reaction is given by the change in the Gibbs Free Energy of polymerization at standard conditions, an expression that can be reduced to:

$$-RT\ln K = \Delta G_p^\circ = \Delta G(M) - \Delta G_{std}^\circ \tag{2}$$

For a ternary system with monomer, polymer and solvent present, the change in Gibbs Free Energy of the monomer is given by:[31]

$$\frac{\Delta G(M)}{RT} = \ln\phi_M + \left(1 - \frac{1}{m}\right)\phi_p + \chi_{Ms}\phi_s^2 + \chi_{Mp}\phi_p^2 + \left(\chi_{Ms} + \chi_{Mp} - \chi_{sp}\right)\phi_s\phi_p \tag{3}$$

where χ_{ij} is the interaction parameter for the various i,j pairs and ϕ_i is a volume fraction. Thus the change in the equilibrium reaction constant, i.e. $1/[M]_{eq}$, is not only a function of temperature, but also of composition.

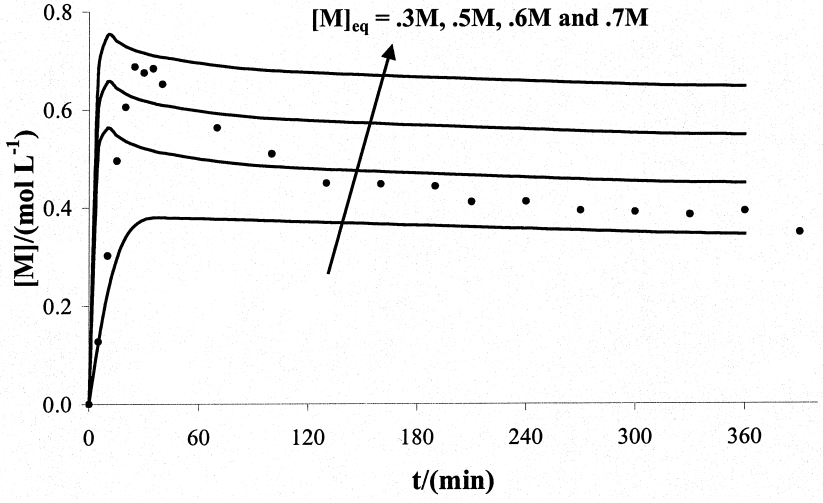

Figure 4. Unreacted monomer concentration profiles computed from eq. 1 for BMA base case semi-batch polymerization at 140 °C with rate coefficients taken from Table 3. Base case experimental data (•). The solid lines represent profiles calculated assuming equilibrium monomer concentrations of 0.3, 0.5, 0.6, and 0.7 mol· L^{-1}.

Table 3. Rate Constants Used in Predici

Taken From Literature:

	Pre-exponential	-E/R
k_p ($L \cdot mol^{-1} \cdot s^{-1}$)	3.80×10^6	2754
k_d (s^{-1})	6.78×10^{15}	17714
$k_{t,tot}$ ($L \cdot mol^{-1} \cdot s^{-1}$)	7.10×10^7	830
C_s	β	4590

Estimated in This Work:

α	0.65	($k_{td} = \alpha k_{t,tot}$)
β	111	
f	0.52	
a_0	1.76×10^6	
a_1	1.37×10^6	

$[M]_{eq} = (a_0 - a_1 x_{wp}) \exp(-6338.8/T)$

A model to test the hypothesis that $[M]_{eq}$ varies with polymer content was developed in Predici®. Rate coefficients are summarized in Table 3. Literature values were used for k_p,[42] k_d,[43] and k_t.[44] Based upon free-volume calculations and the low 50 centipoise solution viscosity of the reaction mass at temperature, k_t was assumed not to vary over the course of the experiment. Other rate coefficients – the chain transfer to xylene constant[45] (C_s, with pre-exponential factor β) and the fraction of termination by disproportionation (α) – were adjusted based on ESI-FTMS and NMR analysis. The

activation energy of the depropagation rate constant was taken from Hutchinson et al.,[23] and the pre-exponential adjusted to fit the base case data. The initiator efficiency f was also adjusted to match the molecular weight profile of the base case experiment.

Figure 5 is a comparison of the predicted unreacted monomer profile for the base case with experimental data using three different treatments of depropagation: $k_{dep} = 0$, $k_{dep} = f(T)$ and $k_{dep} = f(T,x_{wp})$, where x_{wp} is the weight fraction polymer in solution. Without depropagation, the model significantly overpredicts both conversion and molecular weight. The $k_{dep} = f(T)$ model predicts an increase in the free monomer level over the course of the feeds due to the increasing polymerization temperature with time. The decrease in the experimental unreacted monomer content with time, in spite of the increasing reaction temperature, is strong evidence of a decreasing monomer equilibrium constant. Thus, the base case data is best fit by the $k_{dep} = f(T,x_{wp})$ model with $[M]_{eq} = (a_0 - a_1 x_{wp})\exp(-6338.8/T)$, with $a_0 = 1.76\times10^6$ and $a_1 = 1.37\times10^6$. This empirical fit captures the effect of polymer content on the thermodynamic equilibrium; future work will attempt to capture this effect via the interaction parameters in eq. 3.

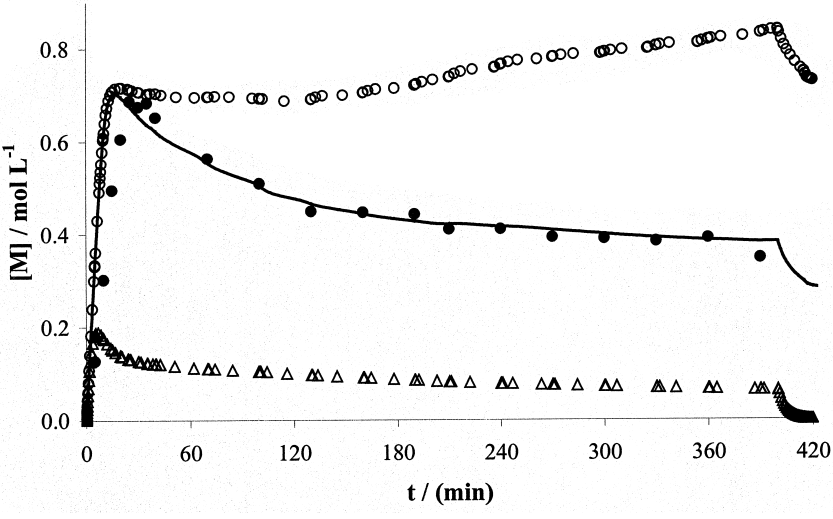

Figure 5. Comparing three different ways of modeling depropagation kinetics of BMA against experimental base case results (•). Model with: $k_{dep} = 0$ (Δ); $k_{dep} = f(T)$ (o); $k_{dep} = f(T, x_{wp})$ (——).

The $k_{dep} = f(T,x_{wp})$ model was used to predict unreacted monomer concentration profiles for the other cases without further parameter adjustment. As seen in Figure 6, the model correctly predicts the increase in unreacted monomer concentrations for the low polymer content experiment. It also makes a reasonable prediction of the resulting molecular weights for both cases, as shown in Figure 7. The model is offset from M_w experimental results most early in the run, but the overall trends are well-captured. The depropagation model also successfully represents the 180 minute experiments, as well as data obtained in a continuous stirred reactor, as will be detailed in a later publication. Including the effect of polymer concentration on methacrylate propagation – depropagation equilibrium is essential to the accurate prediction of the conversion and molecular weight profiles.

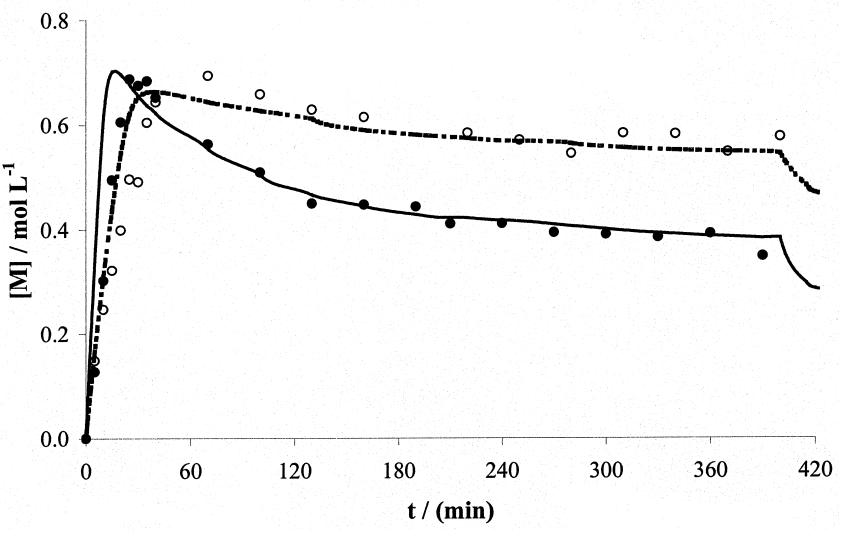

Figure 6. Unreacted monomer concentration profiles predicted using $k_{dep} = f(T,x_{wp})$ model for BMA experiments with 400 min feed times. 35 weight % monomer experimental data (o) and model prediction (- - -); 70 weight % monomer base case experimental data (•) and model fit (——).

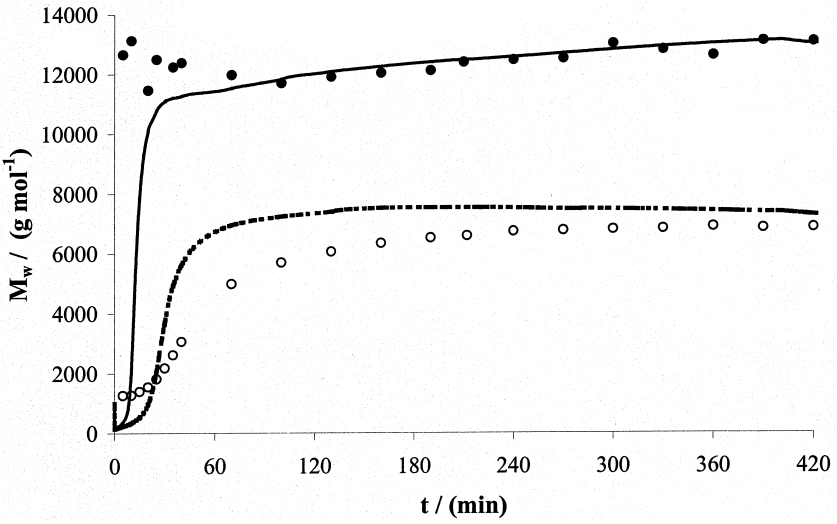

Figure 7. M_w profiles predicted using $k_{dep} = f(T, x_{wp})$ model for BMA experiments with 400 min feed time. 35 wt % monomer experimental data (o) and model prediction (- - -); 70 wt% monomer base case experimental data (•) and model fit (——).

Results of the n-Butyl Acrylate Experiments

A similar series of experiments were carried out in the study of n-butyl acrylate to quantify the impact of the basic process parameters of feed time and polymer content. Shown in Figure 8 are the free monomer profiles for the four cases already described applied to nBA polymerization. It is useful to compare the trends to the BMA experiments. For nBA, the free monomer concentrations are lower than for BMA (no depropagation), and trend proportionally with monomer content: the higher the monomer content in the formula, the higher the free monomer level in the reactor. There is a steep build-up of free monomer at the beginning of the feeds, as the polymerization waits for the radical concentration to reach steady-state. Figure 9 shows the M_w profiles for the experiments. The trends are consistent with the BMA experiments although feed time seems to have more of an impact than in the nBA case. In addition, the absolute values of M_w are lower for the nBA polymerizations than the corresponding BMA cases.

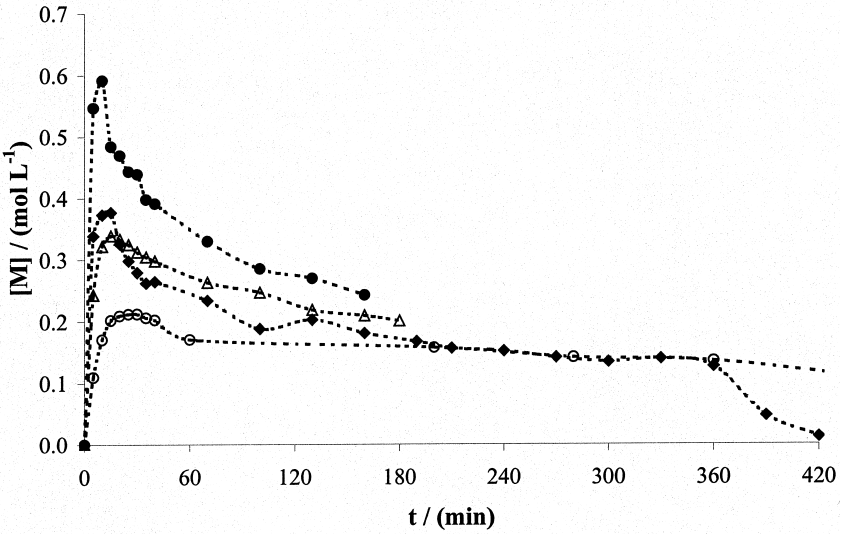

Figure 8. Unreacted monomer profiles of the nBA experiments. 70 wt % monomer, 180 min monomer feed (•); 35 wt % monomer, 180 min feed (Δ); 70 wt % monomer, 400 min feed (♦); 35 wt % monomer, 400 min feed (o). Lines connect experimental points, and do not represent model fits.

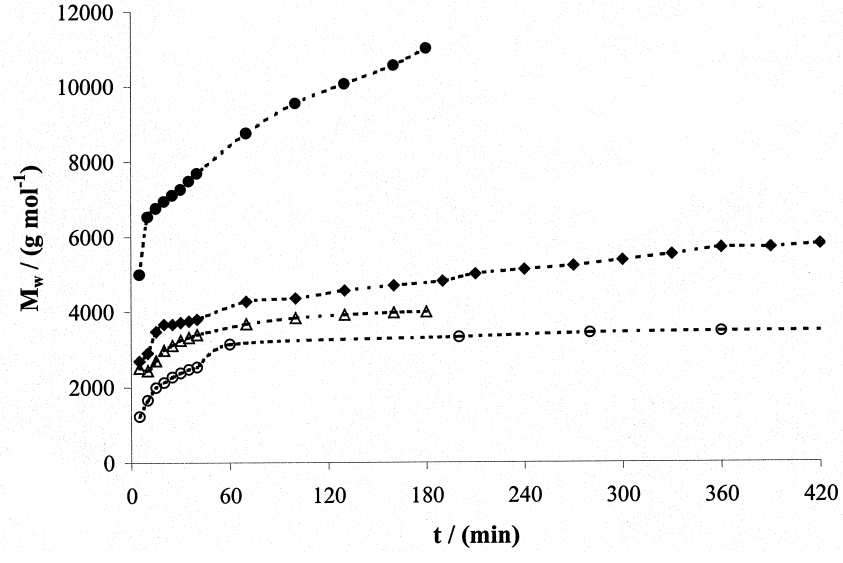

Figure 9. Weight average molecular weight profiles of the nBA experiments. 70 wt % monomer, 180 min monomer feed (•); 35 wt % monomer, 180 min feed (Δ);70 wt % monomer, 400 min feed (♦); 35 wt % monomer, 400 min feed (o). Lines connect experimental points, and do not represent model fits.

Discussion of the nBA Results

A simple polymerization model has been constructed in Predici® using current literature estimates for the kinetic rate coefficients and neglecting H-abstraction and scission reactions. The predicted free monomer profile when using the PLP-determined k_p value significantly overpredicts the conversion of monomer to polymer (underpredicts free monomer left in the reaction mass). Thus, an apparent k_p was determined by fitting the experimental free monomer and M_w data. The fitted k_p was $1/20^{th}$ the value of the PLP value, supporting the view that secondary reactions significantly affect the nBA polymerization rate at these experimental conditions. The slower propagation of mid-chain radicals is one possible explanation for the reduced reaction rate,[26,35-36] and these secondary mechanisms will be included in future modelling efforts. Figure 10 shows the mechanistic pathway for intramolecular H-abstraction followed either by monomer addition or β-scission. Mid-chain radicals can also be formed by intermolecular abstraction (not shown). Monomer addition to the mid-chain radical leads to the formation of a branchpoint that can be measured by ^{13}C NMR spectroscopy. As outlined by Ahmad et al.,[38] branching frequency is estimated from the resonance at 47.6-48.6 ppm arising from the quaternary carbon of the branching point, and from the resonances of the methylene and methine carbons (37-40 ppm) located adjacent to the quaternary carbon. Measurements on poly-BA produced under base-case conditions (70 wt% polymer; 400 min feed time) suggests that between 10-15% of the BA repeat units on the polymer chains are branched. With an number-average DP of 24 (M_n of 3000), this corresponds to 2-4 branchpoints per chain.

ESI-FTMS, with its ability to identify the exact molar mass of low-MW polymeric molecules, is a powerful technique for testing mechanistic arguments providing the proposed structures have unique MW signatures.[40] The β-scission reaction shown in Figure 10 leads to the formation of a macromer terminated chain and a β-scission initiated short-chain radical. These end groups have a unique MW when compared to the other chain-initiating and chain-terminating species identified for this nBA polymerization system (shown in Figure 11). The methyl radical (a) can be formed by fragmentation of the primary oxygen-centered radicals arising from thermal decomposition of the peroxyacetate initiator, either through CO_2 release from the acetoxy radical, or decomposition of the tert-butoxy radical to acetone and the CH_3 radical.[43] In addition, both oxygen-centered radicals may abstract H from the xylene solvent, leading to the formation of the xylol radical (b); the xylol radical can also form

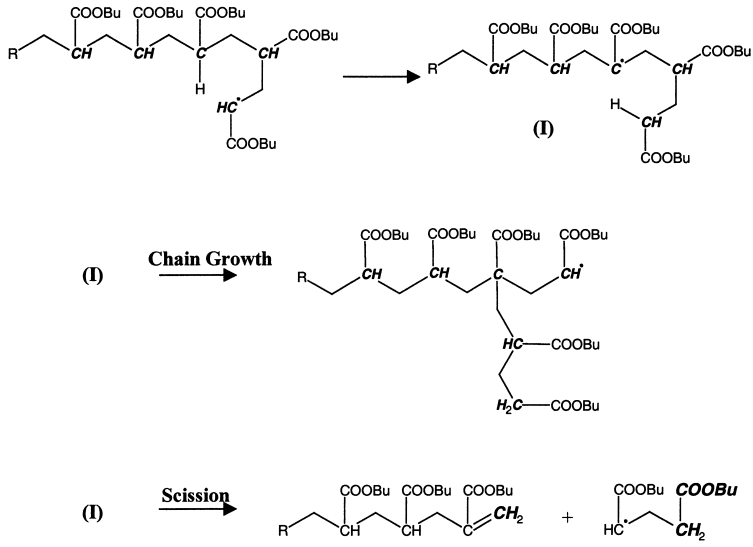

Figure 10. Mechanism of intramolecular H-abstraction to form mid-chain radical (**I**). This radical can undergo monomer addition to create a quaternary C and a short-chain branch, or undergo β-scission to form a macromer-terminated chain and a β-scission initiated short-chain radical.

via H-abstraction by a growing polymer chain. No evidence of tert-butoxy or acetoxy chain-end fragments were found in the analysis of the ESI-FTMS data, indicating that experimental conditions (high temperature, low monomer concentration) favor fragmentation of, or H-abstraction by, these oxygen-centered radicals rather than monomer addition. The terminating chain-ends identified are those formed by H-abstraction (d) and the macromer end (e) formed by β-scission.

An nBA chain consisting of 9-repeat units initiated by a methyl radical and terminated by H-abstraction will have a MW of 1169 (15.07+9×128.08+1.01). The addition of the Na^+ added to the chain during ionization shifts this peak to 1192. A peak of this exact MW is found in the ESI spectrum, as shown in Figure 12. The two peaks immediately following (1193 and 1194) are isotopes of this same structure, whose intensities can be calculated based upon the natural abundance of ^{13}C. The next major peak, occurring at 1204, can be uniquely attributed to a methyl-initiated macromer-terminated chain containing 9 nBA repeat units. Figure 12 shows all of the peaks found in a MW range corresponding to one nBA repeat unit, between the CH_3-$(nBA)_9$-H and CH_3-$(nBA)_{10}$-H signals. The spectrum is for a poly-nBA sample produced with 70 wt % monomer and a 400 min feed time, and was obtained using only the lower MW poly-nBA species

eluting from GPC fractionation to eliminate signals from multiple-charged higher MW species.[40] Full details of the ESI-FTMS analysis and the peak assignments will be provided in a later publication.

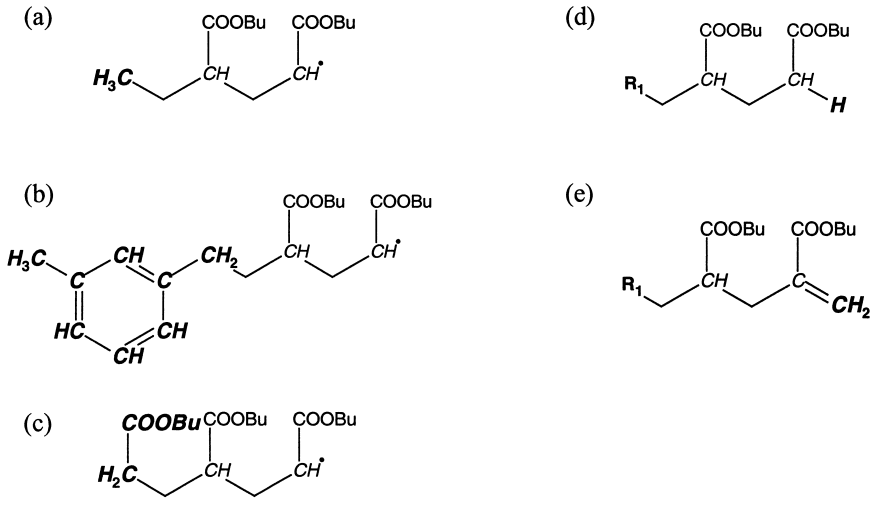

Figure 11. Most abundant nBA polymer end-group structures identified by ESI-FTMS spectra. (a)-(c) are chain-initiating structures formed from: (a) CH3 radical (MW=15); (b) xylol radical (MW=105); (c) β-scission radical (MW=115). The majority of chains are terminated via (d) H-abstraction (MW=1) or (e) β-scission leading to macromer formation (MW=12).

All of the major peaks and many of the minor ones in the ESI-FTMS spectrum have been identified as indicated on Figure 12, and assigned to chain structures containing the end groups shown in Figure 11. The presence of significant amounts of β-scission initiated and macromer terminated structures indicate that chain scission is an important mechanism in this system. Note that although the chain ends formed by scission can be readily identified using ESI-FTMS, the presence of short-chain branches cannot: as seen by examining Figure 10, the MW of the branched structure is the same as that of a linear structure containing the same total number of nBA repeat units. Information from the two techniques (^{13}C NMR and ESI-FTMS) must be combined in order to obtain the detailed picture of polyacrylate chain structure needed to elucidate the relative importance of the competing branching and scission mechanisms.

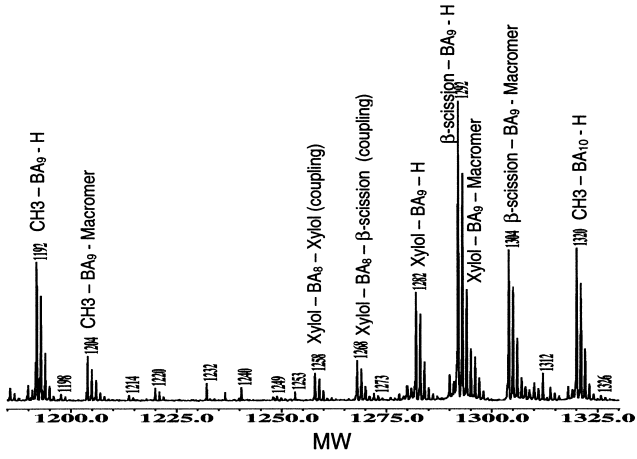

Figure 12. ESI-FTMS spectrum of low MW polymer fraction for nBA polymerization with 70 wt % monomer and 400 minute feed time. All species are singly charged; the indicated MW is that of the sodiated polymer chain. Chain-end structures are shown in Figure 11.

Summary and Future Work

Higher temperature polymerization of methacrylates and acrylates involve the additional mechanisms of depropagation and back-biting followed by beta-scission or branch formation. The equilibrium concentration for the propagation-depropagation free-radical polymerization of n-butyl methacrylate is shown to be dependent on both temperature and polymer composition. This added dependence properly explains the influence of polymer content on MW over the course of a methacrylate polymerization. Future work will be to extend this study to other alkyl methacrylates while extending the theoretical thermodynamic treatment.

The n-butyl acrylate polymerization results are consistent with other recent work hypothesizing that the formation of mid-chain radicals by H-abstraction is responsible for a significant reduction in the effective propagation rate of the system. Moreover, the detailed ^{13}C NMR spectroscopy and ESI-FTMS analyses identify the presence of high levels of branched structures and end groups attributable to β-scission. Not only is scission an important MW-controlling mechanism, the resulting acrylate macromers are available for radical attack and incorporation into another growing chain. Further analytical work is needed to quantify the relative importance of branching and scission, and to capture the behavior of these systems in quantitative models.

The focus of this paper was to understand the role of secondary mechanisms in the homopolymerizations of n-butyl methacrylate and n-butyl acrylate. In future, the more important question of how these mechanisms will influence copolymerizations involving methacrylates and acrylates will also be considered.

Acknowledgements

The authors thank Dr. Joan E. Hansen of DuPont Marshall Laboratory for assistance with the NMR analysis, Dr. Atish Sen and Mr. Ray Celikay for assistance with the electrospray FTMS results, and DuPont Marshall Laboratory for supporting the work.

References

[1] Superintendent of Documents, Title 1, US Government Printing Office, Washington, DC, **1990**, p.1.
[2] Superintendent of Documents, Clean Air Act Amendments of 1990, Title 111, US Government Printing Office, Washington, DC, **1990**, p. 236.
[3] R.S. Reisch, *Chem. Eng. News* **1993**, *71* (October), 34.
[4] K.R. Schultz, *Proc. Adv. Coat. Technol. Conf.*, Chicago, IL, **1992**.
[5] VOC's Directive, *EU Committee of the American Chamber of Commerce in Belgium*, ASBL/VZw, Brussels, July 8, **1996**.
[6] K. Adamsons, G. Blackman, B. Gregorovich, Li Lin, R. Matheson, *Progress in Organic Coatings* **1998**, *34*, 64.
[7] J.W. Prane, *Introduction to Polymers and Resins*, Federation of Societies for Coatings Technology, Philadelphia, PA **1986**, p. 24.
[8] A.S. Balchan, J.A. Klein and F.G. Klein, Loss Prevention and Safety Promotion in the Process Industries, Antwerp, Belgium, **1**, **1995**, p. 1-14.
[9] J. Chiefari, Y.K. Chong, F. Ercole, J. Kristina, T.P. Le, R.T.A. Mayadunne, G.F. Meijs, G. Moad, C. Moad, E. Rizzardo, S.H. Thang, *Macromolecules* **1998**, *31*, 5559.
[10] B.B. Wayland, S. Mukerjee, G. Poszmik, D.C. Woska, L. Basickes, A.A. Gridnev, M. Fryd, S. D. Ittel, in Controlled Radical Polymerization, *ACS Symposium Series 685*, ed K. Matyjaszewski, American Chemical Society, Washington, DC, p. 305-315, **1998**.
[11] M.K. Georges, R.P.N. Veregin, P.M. Kazmaier, G.K. Hamer, *Macromolecules* **1993**, *26*, 2987.
[12] S.J. Wang, K. Matyjaszewski, *Macromolecules* **1995**, *28*, 7901.
[13] R.B. Mesrobian, A.V. Tobolsky, *J. Polymer Sci.* **1947**, *2*, 463.
[14] M. Hakim, V. Verhoeven, N.T. McManus, M.A. Dubé, A. Penlidis, *J. Appl. Poly. Sci.* **2000,** *77*, 602.
[15] K.E. Russell, A.V. Tobolsky, *J. Am. Chem. Soc.* **1953**, *75*, 5052.
[16] F.R. Mayo, *J. Am. Chem. Soc.* **1953**, *75*, 6133.
[17] M. Stickler, G. Meyerhoff, *Makromol. Chem.* **1980**, *181*, 131; ibid. p. 913.
[18] G.T. Russell, D.H. Napper, R.G. Gilbert, *Macromolecules* **1988**, *21*, 2141.
[19] C. Peinado, A. Alonso, F. Catalina, W. Schnabel, *Macromol. Chem. Phys.* **2000**, *201*, 1156.
[20] R. Sack, G.V. Schulz, G. Meyerhoff, *Macromolecules* **1988**, *21*, 3345.
[21] G. Moad, D.H. Solomon, *Aust. J. Chem.* **1990**, *43*, 315.
[22] K.J. Ivin, *J. Polymer Sci.: Part A: Polym. Chem.* **2000**, *38*, 2137.
[23] R.A. Hutchinson, D.A. Paquet Jr., S. Beuermann, J.H. McMinn, *Ind. Eng. Chem. Res.* **1998**, *37*, 3567.
[24] F.S. Dainton, K.J. Ivin, *Nature* **1948**, 705.
[25] J. Chiefari, J. Jeffery, R.T.A. Mayadunne, G. Moad, E. Rizzardo, S.H. Thang, *Macromolecules* **1999**, *32*, 7700.
[26] C. Plessis, G. Arzamendi, J.R. Leiza, H.A.S. Schoonbrood, D. Charmot, J.M. Asua, *Macromolecules* **2000**, *33*, 4 .
[27] F.S. Dainton, K.J. Ivin, *Proc. Roy. Soc. A* **1952**, *212*, 207.
[28] F.S. Dainton, K.J. Ivin, *J. Quart. Rev. Chem. Soc.* **1958**, *12*, 61.
[29] S. Bywater, *Trans. Faraday Soc.* **1955**, *51*, 1267.
[30] P.A. Small, *Trans. Faraday Soc.* **1953**, *49*, 441.

[31] R.L. Scott, *J. Chem. Physics* **1949**, *17*, 268.
[32] R.D. Snow, F.E. Frey, *Ind. & Eng. Chem.* **1938**, *30*, 176.
[33] H. Sawada, *Thermodynamics of Polymerization*, Marcel-Dekker, NY, **1976**.
[34] S. Beuermann, D.A. Paquet Jr., J.H. McMinn, R.A. Hutchinson, *Macromolecules* **1996**, *29*, 4206.
[35] A. M. van Herk, *Macromol. Rapid Commun.* **2001**, *22*, 29.
[36] B. Yamada, M. Azukizawa, H. Yamazoe, D.J.T. Hill, P.J. Pomery, *Polymer* **2000**, *41*, 5611.
[37] E.F. McCord, W.H. Shaw Jr., R.A. Hutchinson, *Macromolecules* **1997**, *30*, 246.
[38] N. M. Ahmad, F. Heatley, P. A. Lovell, *Macromolecules* **1998**, *31*, 2822.
[39] K.F. O'Driscoll, A.F. Burczyk, *Polym. React. Eng.* **1992-93**, *1*, 111.
[40] D. J. Aaserud, L. Prokai, W. J. Simonsick Jr., *Anal. Chem.* **1999**, *71*, 4793.
[41] J.M. Prausnitz, R.N. Lichtenthaler and E.G. de Azevedo, *Molecular Thermodynamics of Fluid-Phase Equilibria, 2nd Ed.*, Prentice-Hall Inc., Englewood Cliffs, NJ, **1986**, p. 306-316.
[42] S. Beuermann, M. Buback, T.P. Davis, R.G. Gilbert, R.A. Hutchinson, A. Kajiwara, B. Klumperman, G.T. Russell, *Macromol. Chem. Phys.* **2000**, *201*, 1355.
[43] M. Buback, S. Klingbeil, J. Sandmann, M.-B. Sderra, H.P. Vögele, H. Wackerbarth, L. Wittkowski, *J. Phys. Chem. (Munich)* **1999**, *210*, S199.
[44] M. Buback, C. Kowollik, *Macromol. Chem. Phys.* **2000**, *200*, 1764. M. Buback, C. Kowollik, *Macromolecules* **1999**, *32*, 1445.
[45] P.V.T. Raghuram, U.S. Nandi, *J. Polym. Sci: Part A-1* **1970**, *8*, 3079.